



# Engineered living materials grown from programmable *Aspergillus niger* mycelial pellets



Ke Li<sup>a,1</sup>, Zhen Wei<sup>b,1</sup>, Jianyao Jia<sup>a</sup>, Qing Xu<sup>a</sup>, Hao Liu<sup>b,c,\*</sup>, Chao Zhong<sup>d,e,\*\*</sup>, He Huang<sup>a,\*\*\*</sup>

<sup>a</sup> School of Food Science and Pharmaceutical Engineering, Nanjing Normal University, Nanjing, 211816, China

<sup>b</sup> MOE Key Laboratory of Industrial Fermentation Microbiology, College of Biotechnology, Tianjin University of Science & Technology, Tianjin, 300457, China

<sup>c</sup> Tianjin Engineering Research Center of Microbial Metabolism and Fermentation Process Control, Tianjin University of Science & Technology, Tianjin, 300457, China

<sup>d</sup> Center for Materials Synthetic Biology, Shenzhen Institute of Synthetic Biology, Shenzhen Institutes of Advanced Technology, Chinese Academy of Sciences, Shenzhen, 518055, China

<sup>e</sup> CAS Key Laboratory of Quantitative Engineering Biology, Shenzhen Institute of Synthetic Biology, Shenzhen Institutes of Advanced Technology, Chinese Academy of Sciences, Shenzhen, 518055, China

## ARTICLE INFO

### Keywords:

Engineered living material  
Filamentous fungus  
*Aspergillus niger*  
Genetic circuit  
Melanin

## ABSTRACT

The development of engineered living materials (ELMs) has recently attracted significant attention from researchers across multiple disciplines. Fungi-derived ELMs represent a new type of macroscale, cost-effective, environmentally sustainable materials. However, current fungi-based ELMs either have to undergo a final process to heat-kill the living cells or rely on the co-culture with a model organism for functional modification, which hinders the engineerability and versatility of these materials. In this study, we report a new type of ELMs – grown from programmable *Aspergillus niger* mycelial pellets – by a simple filtration step under ambient conditions. We demonstrate that *A. Niger* pellets can provide sufficient cohesion to maintain large-area self-supporting structures even under low pH conditions. Subsequently, by tuning the inducible expression of genes involved in melanin biosynthesis, we verified the fabrication of self-supporting living membrane materials with tunable colors in response to xylose concentration in the surroundings, which can be further explored as a potential biosensor for detecting xylose level in industrial wastewater. Notably, the living materials remain alive, self-regenerative, and functional even after 3-month storage. Thus, beyond reporting a new engineerable fungi chassis for constructing ELMs, our study provides new opportunities for developing bulk living materials for real-world applications such as the production of fabrics, packaging materials, and biosensors.

## 1. Introduction

For billions of years, living systems have constantly been evolving to produce diverse, complex materials under ambient conditions (from biofilms to skeletal tissues) that have acquired remarkable properties such as hierarchical assembly from simple raw materials, self-repairing, and the ability to sense and respond to environmental stimuli [1–5]. There is tremendous potential for exploiting different forms of engineered living materials (ELMs) to recapitulate the unique “living” attributes of natural living systems. Existing ELMs reported thus far include

two basic categories, hybrid living materials and self-organizing ones [6, 7]. The former generally requires the use of an extra matrix such as hydrogel, organic coating, and inorganic material in which living cells are embedded. The introduction of these exogenous scaffolds often affects the ability of cells to perceive the external environment, which restricts their living abilities [8–11]. Moreover, these ELMs face several major obstacles, including the complex processing steps and associated high manufacturing costs [12,13]. Alternatively, self-organizing living materials are produced by harnessing engineered cells to simultaneously make the matrix and incorporate novel functionalities into it [4,6,9,10,

\* Corresponding author. MOE Key Laboratory of Industrial Fermentation Microbiology, College of Biotechnology, Tianjin University of Science & Technology, Tianjin, 300457, China.

\*\* Corresponding author. Center for Materials Synthetic Biology, Shenzhen Institute of Synthetic Biology, Shenzhen Institutes of Advanced Technology, Chinese Academy of Sciences, Shenzhen, 518055, China.

\*\*\* Corresponding author.

E-mail addresses: [liuhao@tust.edu.cn](mailto:liuhao@tust.edu.cn) (H. Liu), [chao.zhong@siat.ac.cn](mailto:chao.zhong@siat.ac.cn) (C. Zhong), [huangh@nju.edu.cn](mailto:huangh@nju.edu.cn) (H. Huang).

<sup>1</sup> These authors contributed equally to the work.

<https://doi.org/10.1016/j.mtbio.2023.100545>

Received 6 November 2022; Received in revised form 3 January 2023; Accepted 5 January 2023

Available online 14 January 2023

2590-0064/© 2023 Published by Elsevier Ltd. This is an open access article under the CC BY-NC-ND license (<http://creativecommons.org/licenses/by-nc-nd/4.0/>).

14]. Compared with existing self-organizing living materials that often use model bacterial strains, such as *Escherichia coli* and *Bacillus subtilis*, as the main chassis, the use of other microorganisms, such as fungi, is relatively less explored even though they have exhibited great potential to produce self-organizing bulk materials without supplementation of extra scaffolding materials [15–18].

The relatively high aspect ratios of the filaments in fungi render them particularly suitable as prime candidates for fabricating sheet-like structures or membranes, or even for application as a reinforcing phase in composite materials [15]. Indeed, researchers have already reported the generation of fungal-based materials as scalable biocomposites, including packaging materials, bio-bricks, and leathers [16,17,19]. These studies showed considerable promise in the fabrication of living materials using fungal mycelium. However, these materials either have to undergo a final process to heat-kill the living cells or rely on the co-culture with a model organism for functional modification [19–22], severely limiting the engineerability and versatility of fungi-based ELMs.

Here, we report the fabrication of new fungal ELMs that leverage *Aspergillus niger* as an engineerable chassis. *A. niger* is a filamentous fungus that primarily comprises a vast three-dimensional network of web-like hyphae, forming a complex and well-ordered structure. Moreover, it is genetically tractable, thus rendering it an ideal chassis for use in ELMs [23,24]. In this study, using a simple filtration step, we first produced self-supporting living membrane materials composed of *A. niger* mycelial pellets. We further reconstructed the intrinsic melanin pigment synthesis pathway of *A. niger* to fine-tune the expression levels of melanin, leading to living membrane materials with variable colors. Our results not only provide a new viable chassis for constructing bulk ELMs with tunable colors but also open a new avenue for realizing many real-world applications, such as the production of fabrics, packaging materials, and biosensors.

## 2. Material and methods

### 2.1. Strains and culture conditions

*A. niger* wild type ATCC1015 was purchased from the Microbial Species Preservation Center (Guangdong, China). All the wild type and mutant strains were cultivated in complete medium (CM) or potato dextrose agar (PDA). Conidia of  $1 \times 10^8$  for each strain were inoculated in a 250-mL Erlenmeyer flask. The medium was composed of 100 g/L glucose, 80 g/L CaCO<sub>3</sub>, 6 g/L Bacto Peptone, 150 mg/L KH<sub>2</sub>PO<sub>4</sub>, 150 mg/L K<sub>2</sub>HPO<sub>4</sub>, 100 mg/L MgSO<sub>4</sub>·7H<sub>2</sub>O, 100 mg/L CaCl<sub>2</sub>·2H<sub>2</sub>O, 5 mg/L FeSO<sub>4</sub>·7H<sub>2</sub>O, and 5 mg/L NaCl.

### 2.2. Plasmids construction

Using pLH594 as the parent vector, the same strategy as reported previously was used to construct the 4' phosphopanthetheinyl transferase (pptA) deletion plasmid pLH773 [23]. Briefly, the upstream and downstream sequences (~1 kb) of the pptA (ANI\_1\_1720104) encoding region were amplified with primers PpPtA-up-F/PpPtAup-R and PpPtA-down-F/PpPtA-down-R, respectively. The corresponding sequences were digested and ligated sequentially to the flanks of the hygromycin resistance cassette (loxP-hph-loxP) in pLH594 to obtain the pptA-deletion plasmid pLH773.

To construct pptA overexpression plasmid, pLH454 harboring glyceraldehyde-3-phosphate dehydrogenase promoter (PgpdA) and loxP-hph-loxP cassette as previously described, was used as the parent vector, the plasmid pLH774 derived from pLH454 by replacement of PgpdA with the pptA gene, which does not contain a promoter, was designed. The promoter of the xylanase A gene (Pxyn) was cloned into pLH774 to obtain plasmid pLH777 with primer Pxyn-F/Pxyn-R. The primers used are listed in Table S1, plasmids and strains used in this study are listed in Table S2, and the map of plasmids is shown in Fig. S1.

### 2.3. Transformation of *A. niger*

The plasmids were electrotransformed into *Agrobacterium tumefaciens* [25]. A total of  $2 \times 10^6$  of *A. tumefaciens* cells containing the plasmid and *A. niger* conidia were co-cultured on IM solid medium plate supplemented with 0.2 M acetosyringone (AS) and 100 µg/mL kanamycin at 23 °C for 2 days. Then, the mixture was transferred onto CM plates supplemented with hygromycin B (250 µg/mL), cefotaxime (200 µM), ampicillin (100 µg/mL), and streptomycin (100 µg/mL) until colonies appeared.

### 2.4. Gene deletion and overexpression of *A. niger*

The pptA-deletion plasmid pLH773 was introduced into *A. niger* strain S469 via AMT. Transformants were selected on CM supplemented with ampicillin (100 µg/mL), streptomycin (100 µg/mL), cefotathiazide sodium (100 µg/mL), and hygromycin B (250 µg/mL) at 28 °C for 5 days, and the pptA-deletion event was determined by PCR analysis using primers P1/P2 and P3/P4.

The plasmid containing pptA with Pxyn promoter was introduced into  $\Delta$ pptA by AMT. Transformants were selected on CM plates as described above. The gene integration events were confirmed by PCR analysis using primer P5/P6. All plasmids and strains in this study are listed in Table S1.

### 2.5. DPPH/ABTS radical scavenging activity

DPPH/ABTS radical scavenging activity was measured with a commensurable test kit (Beijing Solarbio Science & Technology Co., Ltd.). The mixture of samples and DPPH was allowed to stand at room temperature in the dark for 30 min. Then the absorbance of the resulting solution was measured at 517 nm (DPPH) or 734 nm (ABTS). A lower absorbance indicates higher free radical scavenging activity. The DPPH/ABTS radical scavenging activity of each sample was calculated as the percent inhibition according to the following equations.

where  $A_{\text{negative control}}$  represents the absorbance (A) of the sample and absolute ethyl alcohol,  $A_{\text{blank}}$  represents the absorbance (A) of double distilled water and testing buffer in the kit.

### 2.6. Characterization

Scanning electron microscopy (SEM) images were taken with a Carl Zeiss Supra 40 field emission scanning electron microscope at an acceleration of 5 kV. Fourier-transform infrared attenuated total reflection-Fourier transform infrared (ATR-FTIR) spectroscopy. Spectra were recorded from 4000 to 800 cm<sup>-1</sup> using a nominal resolution of 2 cm<sup>-1</sup> with Spectrum Two™ (PerkinElmer). UV-Visible absorption spectra were obtained on a UV-3600i Plus UV-Vis spectrophotometer (Shimadzu, Japan).

### 2.7. Fabrication of living membrane materials

Spores of *A. niger* were placed on a PDA for 2 days and then cultured in potato dextrose water (PDW, 10<sup>6</sup> CPU/mL) inside a lab shaker (120 rpm, 25 °C) for 76 h. About 300 mg of cells were vacuumed and washed using distilled water three times to remove residual media. The slurry was placed on a glass slide to obtain the living membrane materials after water evaporation under ambient conditions (25 °C, 1 h) until a constant weight was achieved.

### 2.8. Mechanical analysis of living membrane materials

The thickness of the resulting materials was measured at three points along the axis of the sample using a digital length gauge device. Sample weight was measured after tensile tests performed at room temperature with a CMT6103 (MTS, USA) using a preload force of 0.25 N with a 2 mm min<sup>-1</sup> test speed. The bulk density was calculated by dividing the weight of the specimen by the bulk volume of the sample. Young's

modulus (in MPa) was determined at the linear part of the stress/strain curve. The ultimate tensile strength ( $\sigma$ ; MPa) was obtained from the maximum load (N) per unit area ( $\text{mm}^2$ ) of the specimen, while strain at failure ( $\epsilon$ ; %) was obtained by calculating the strain (mm) at the moment of breaking.

## 2.9. TG-DSC analysis

TG analysis was conducted using a simultaneous NETZSCH instrument (STA 449F3, D.E.). A finely ground sample was placed in a platinum crucible and was heated from room temperature to 1000 °C at 10 °C  $\text{min}^{-1}$  under flowing air at 100 mL  $\text{min}^{-1}$ . The weight loss curve of each sample was recorded by the TG analyzer. Differential scanning calorimetric (DSC) curves were simultaneously collected by an online computer and data processing system.

## 3. Results

### 3.1. Rational selection of an ideal chassis for the design of a living membrane material

*Aspergillus niger*, a group of black aspergilli, is “generally regarded as safe” (GRAS) [26]. In contrast with *E. coli*, *B. subtilis*, and other chassis cells commonly used for producing living materials, *A. niger* could grow under a wide range of temperatures (6–47 °C) and pH values (1.5–9.8) [26]. To date, *A. niger* has been modified into a cell factory to produce a wide range of valuable molecules (U.S. Food and Drug Administration) [27]. Variable efficient genetic manipulation tools have been developed for enhancing protein expression in *A. niger*, making it a new suitable chassis for fabricating ELMs.

Like other filamentous fungi, *A. niger* is capable of growing into mycelial pellets under shaking conditions (Fig. 1A). The cell walls of these pellets are composed of polysaccharides, including chitin and  $\alpha$ / $\beta$ -glucans, and glycosylated proteins, which result in a high dipole moment and strong hydrogen bonding, and make it an ideal species to construct bulk living materials [28,29]. Strengthening this material-forming ability of *A. niger* cells would not only reduce the need for exogenous scaffolding materials but also enable direct contact between materials and the environment, reducing the waste of energy and resources caused by redundant processing steps (Fig. 1B).

In addition, our key observation is that *A. niger* is one of the main carriers of fungal melanin pigments. Its conidia can produce olive-brown to black pigment molecules. The production of dihydroxynaphthalene (DHN) melanin by *A. niger* is regulated by the melanin biosynthesis gene cluster, which contains genes *pksP*, *ayg1*, *arp1*, *arp2*, and *abr2*. The *pksP* gene is the core gene responsible for the first biosynthetic step of YWA1 (heptaketide naphthopyrone, 2,5,6,8-tetrahydroxy-2-methyl-2,3-dihydro-4H-naphtho(2,3- $\beta$ ) pyran-4-one) from the substrates, acetyl-CoA and malonyl-CoA [30,31]. Notably, the enzymatic activity of polyketide synthases (PKS) requires post-translational modification, which was performed by a specific member of the 4-phosphopantetheinyl transferase (PPTase) family. We focused our engineering efforts on DHN melanin because it is well known for its variation in color from pale beige to dark brown as the yield changes and its production does not disrupt fungal growth (Fig. 1C). Utilizing this inner melanin production ability of *A. niger* would avoid the introduction of exogenous genes that potentially causes additional burdens to the host, while simultaneously ensuring the stable release of functional elements in a controllable manner. Collectively, *A. niger*, as a novel chassis, has the potential for the construction of a new type of ELMs. As demonstrated, later on, using a simple vacuum filtration method, we have successfully produced self-supporting membrane materials consisting of dense *A. niger* hyphae as the sole raw material (Fig. 1D).

### 3.2. Fabrication of living membrane materials from *A. niger* mycelia pellets

To verify the ability of *A. niger* cells to produce self-supporting living membrane materials, the reliable production of hyphae under appropriate conditions is an important consideration. *A. niger* serves as a suitable model in this regard because it is capable of utilizing cheap renewable carbon sources and can grow at low pH (<2 pH) [24]. Using a typical protocol for fungal growth by constant shaking, we observed band-like growth of hyphae coming from one side of the spore of *A. niger*, producing branches (Fig. S2). Upon shaking, the hyphae interact with themselves while the cells continue to grow and divide. This interaction between hyphae yielded the formation of a large amount of amorphous fibrous pellets. Next, we examined whether *A. niger* cells could grow normally under different pH conditions (pH 2, 6, 8, and 10). After 3 d of growth, dense pellets covering the entire bottom of the conical flask were observed under all chosen conditions (Fig. 2A and Fig. S3).

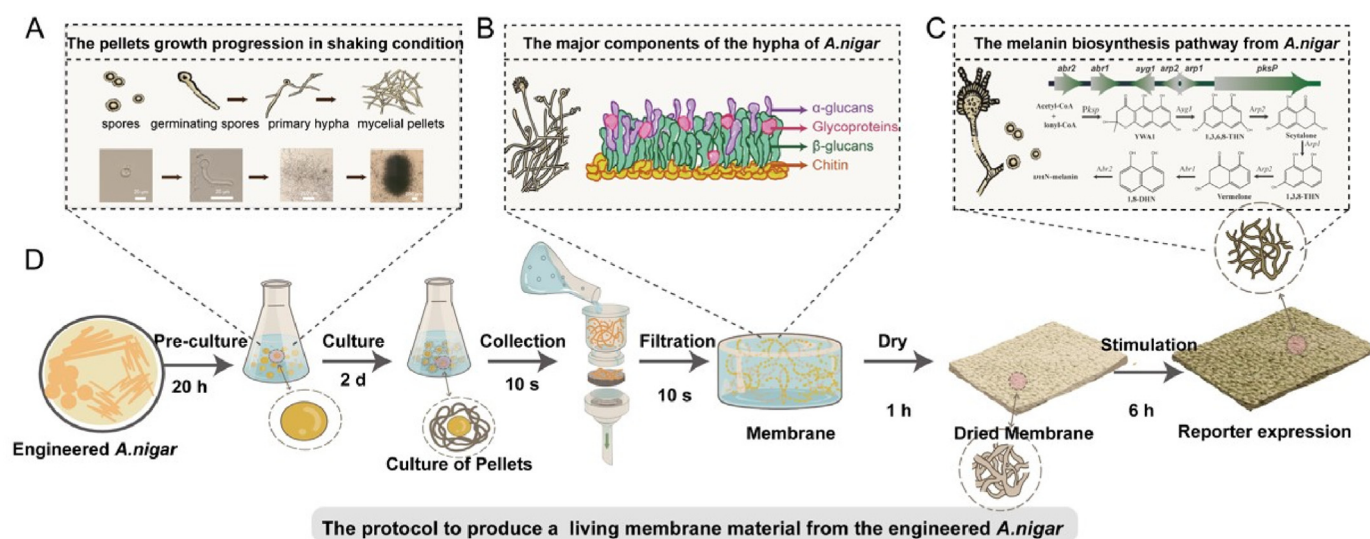


**Fig. 1.** Schematic showing the design and production of a living membrane material grown from *A. niger*. A, Schematic showing the typical steps to produce mycelial pellets from *A. niger* in shaking cultures; B, Schematic showing the major components of the hypha; C, Schematic showing the melanin biosynthesis pathway and genomic organization of the genes involved in melanin biosynthesis; D, The typical protocol to produce a living membrane material grown from the engineered *A. niger*.

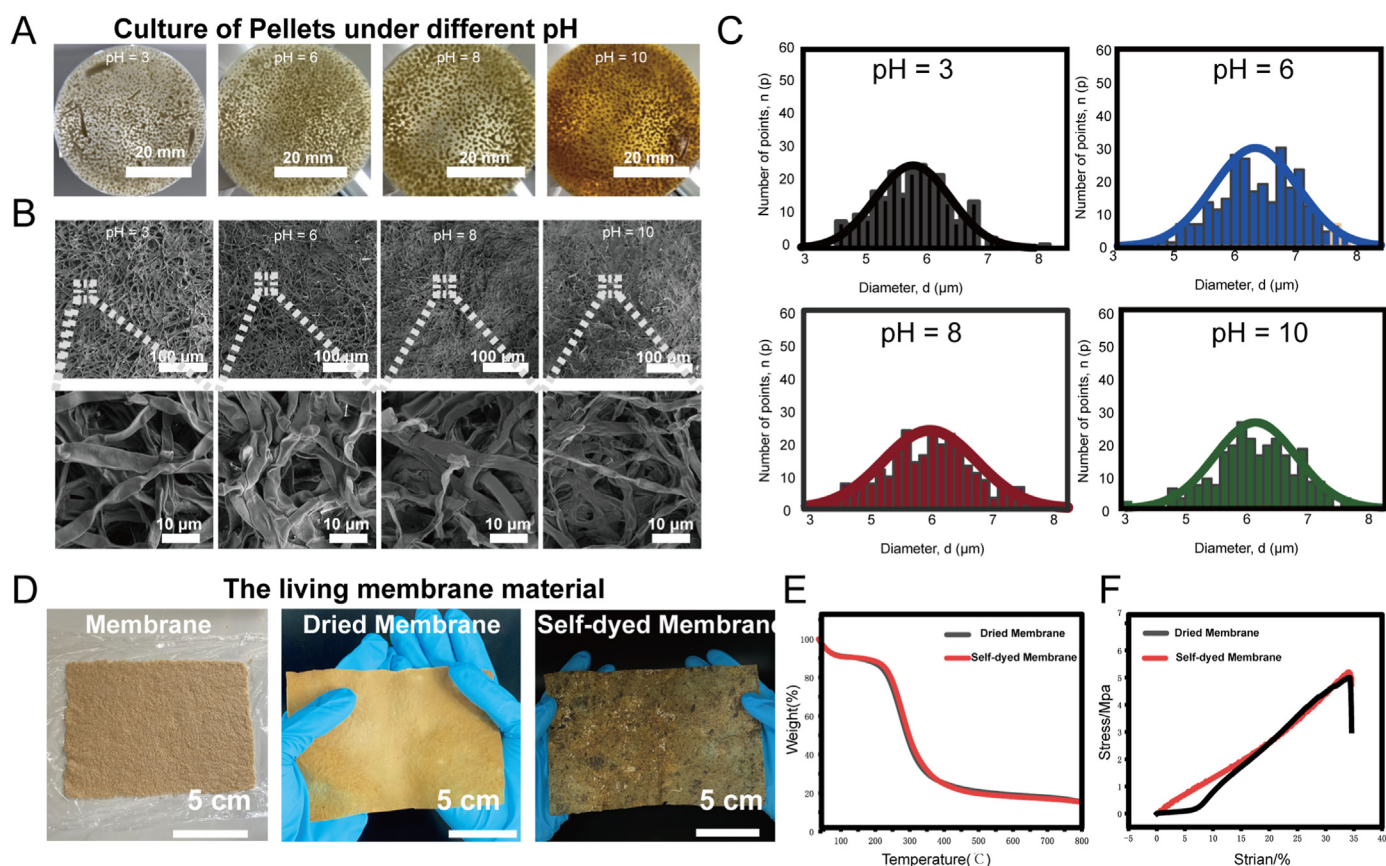


**Fig. 2.** Fabrication of living membrane materials from *A. niger*. A, Representative images of mycelial pellets produced by *A. niger* under different pH conditions; B, SEM images of mycelial pellets produced by *A. niger* under different pH conditions; C, Distribution of hyphal diameters of the living material grown from the Spynx-pptA strain under different pH conditions; D, Typical images of the as-prepared membrane, membrane after drying, and self-dyed membrane; E, TGA thermograms of dried membrane and self-dyed membrane; F, representative stress/strain curves of dried membrane and self-dyed membrane.

The fibrous network morphologies of *A. niger* grown at different pH levels were assessed with SEM imaging (Fig. 2B). Visually, the hyphal structures of the pellets were uniform fibrous structures. In addition, we compared the diameters using ImageJ software based on SEM imaging. The mean diameter of the hyphae was almost equal in size at approximately 5000 nm for all samples obtained at different pH values ( $5749 \pm 76$  nm at pH 2,  $6039 \pm 1036$  nm at pH 6,  $5985 \pm 124$  nm at pH 8, and  $5891 \pm 93$  nm at pH 10). The results aligned with previously reported research (Fig. 2C) [24]. Using a similar approach, the engineered strain could grow normally using different carbon sources and surfactants (Fig. S4, Fig. S5, and Fig. S6). Together, these results suggest the possibilities of growing living materials under different conditions by harnessing *A. niger* strong resistance to various harsh conditions.

We then harvested the *A. niger* pellets as building blocks to fabricate living membrane materials. The pellets were filtered and washed with deionized water to remove the media, then dried at room temperature (25 °C) for 1 h until reaching a constant weight (see methods). Once dried, the pellets molded into a cuboid formed a flexible and self-supporting structure (Fig. S7). We considered this dried, solidified structure as a living membrane material. The melanin is synthesized in conidia of *A. niger*, and conidiation hardly takes place in liquid-submerged culture [32]; therefore, we induce self-dying after drying to confirm whether the *A. niger* pellets in the membrane materials remained viable. Intriguingly, the *A. niger* pellets in the membrane materials remain metabolically active throughout the growth and desiccation phases, as they are able to produce melanin pigments even after 6 h incubation on a PDA plate, resulting in a self-dyed living membrane material with tunable colors due to expression of melanin pigments (Fig. 2D).

The thermal behavior of living materials can be a critical factor in many applications, especially those conducted at high or variable temperatures. Therefore, we next examined the thermal behaviors of the living membrane materials, including the non-dyed and self-dyed samples, by thermogravimetric. The data and corresponding curves (Fig. 2E) show that both samples began to degrade at temperatures above 200 °C. In stage 1 of the degradation test (between 25 °C and 200 °C), a 5% weight loss was obtained, attributed to the free and chemically bonded water, mainly between 100 °C and 150 °C. In stage 2 (between 200 °C and 375 °C), we observed a much greater weight loss (~80%), presumably due to the decomposition of organic constituents, such as proteins and the polysaccharide chitin. DSC analysis of the sample revealed glass transitions at approximately 180 °C. Next, we assessed Young's modulus of the samples. The results showed Young's modulus of 1.9 MPa (Fig. 2F). Notably, no significant difference in the thermostability and mechanical properties between the non-dyed and self-dyed membrane materials was detected, implying that the melanin pigment production does not affect those properties.

Collectively, these results demonstrate that the *A. niger* mycelial pellets can serve as building blocks for fabricating self-supporting interconnected living membrane materials with impressive thermal stability.

### 3.3. Construction of living membrane materials with tunable colors grown from engineered *A. niger*

*A. niger* is a melanin-producing fungal species [30]. We demonstrated that living membrane materials made of wild type *A. niger* cells could be self-dyed owing to their innate melanin production capacity. We next attempted to achieve the tunable color of the living materials by

regulating melanin expression. To avoid interference from intrinsic melanin production, we first established a melanin auxotrophic strain. We used the *pptA*-deleted (the PPTase-encoding gene) plasmid, which contained a hygromycin B resistance gene (*hph*) for a selection marker. This plasmid was used to transform an *A. niger* strain (S469) that we had previously constructed. The S469 strain was constructed with a Tet-on-cre-pyrG system in *A. niger* [23,24]. The final transformed *A. niger* strain containing the *pptA*-deleted plasmid was named  $\Delta$ pptA. To further develop the *A. niger* strain as a biosensor that responds to environmental stimuli and triggers changes in gene expression, vectors with promoter and *pptA* genes were constructed and integrated into the  $\Delta$ pptA strain. We selected an inducible system in which xylose triggers the activation of transcription from a target promoter (P<sub>xyn-pptA</sub>). The resulting strain was referred to as Sp<sub>xyn-pptA</sub> (Fig. 3A). Consistent with our design, the pellicles grown from the wild type,  $\Delta$ pptA, and Sp<sub>xyn-pptA</sub> strains were screened for melanin production. While pellicles grown with wild type yeast showed a similar gray color, no melanin production was observed from  $\Delta$ pptA, while clear melanin production was observed from Sp<sub>xyn-pptA</sub>. Notably, pellicles grown from Sp<sub>xyn-pptA</sub> produced varied melanin signals when exposed to different xylose concentrations, verifying that xylose serves as an effective inducer to trigger the expression of melanin in the target strain (Fig. 3B).

Further, we performed UV-VIS spectra (200–800 nm) and attenuated total reflection Fourier-transform infrared (ATR-FTIR) spectroscopy to reveal the physiochemical properties of Sp<sub>xyn-pptA</sub>. Besides the 0% xylose-induced Sp<sub>xyn-pptA</sub> pellicle, other pellicles absorbed strongly in the UV region and progressively decreased as the wavelength increased, corresponding to the conspicuous property due to a high degree of conjugation in the molecule (Fig. 3C). ATR-FTIR spectra of proteins (~1550 cm<sup>-1</sup>), lipids (3000–2800 cm<sup>-1</sup>, ~1740 cm<sup>-1</sup>), nucleic acids (1255–1245 cm<sup>-1</sup>), and polysaccharides (1200–900 cm<sup>-1</sup>) were analyzed to characterize the hyphae. Expectedly, all the characteristic components were confirmed in the spectra, indicating that the growth of hyphae was unaffected by the differential production of melanin (Fig. 3D). These results suggest that the two strains can produce melanin, implying that living membrane materials grown from the strains can be self-dyed with tunable colors.

Fungal melanins are also well known for their ability to protect

organisms from high doses of radiation [33,34]. As the strains can produce variable amounts of melanin in response to different xylose concentrations, their ability to scavenge free radicals provides a promising demonstration of the accurate signal response of the strains. Hence, we evaluated their ability to eliminate the radicals 2,2'-azino-bis (3-ethylbenzothiazoline-6-sulfonic acid; ABTS) and 2,2-diphenyl-1-(2,4,6-trinitrophenyl) hydrazyl (DPPH). The inhibition of DPPH/ABTS radicals by different xylose concentrations varied in the induced pellicles. The inhibition percentage of DPPH radicals ranged from 9.3 to 19.2% in 0–0.1 wt % xylose-induced pellicles (Fig. 3E). The results showed that ABTS radical inhibition ranged from 7.5 to 42.5% (Fig. 3F). The efficiency of DPPH/ABTS radical inhibition was compared with that of the wild type with a value of 17.1% and 41.2%, respectively. These results suggest that Sp<sub>xyn-pptA</sub> exhibited tunable antiradical properties. Based on the inducible expression of melanin in these two strains, we also envision that the self-dyed living membrane materials may be harvested as fabrics that can help resist radiation or be used as a biosensor to estimate the concentration of xylose under various environmental conditions.

To this end, we started by vacuuming approximately 300 mg of two kinds of fresh pellets ( $\Delta$ pptA and Sp<sub>xyn-pptA</sub>) into a membrane and washing them with deionized water to remove the media. The samples were then dried at 25 °C for 1 h until a constant weight was reached (Fig. S7). Once dried, both membranes were cultured on a PDA plate containing 0.05% xylose. Visually, the self-supported and flexible membrane composed of different strains ( $\Delta$ pptA and Sp<sub>xyn-pptA</sub>) showed different colors (Fig. 4A and B). SEM imaging (Fig. 4C and D) confirmed that the molded films contained an appreciable quantity of spores, the reproductive cells of fungi. Next, we assessed the mechanical properties, including Young's modulus, flexural modulus, and elongation at the break of the 0.1% xylose-induced and uninduced material, to determine whether melanin pigment production affects these properties. The results demonstrate Young's modulus of 1.8 MPa and flexural modulus of 2.9 MPa, which is similar to that of material-containing wild type cells (Fig. 4E and F). These preliminary results suggest the membrane materials made by the engineered *A. niger* could avoid the interference from intrinsic melanin production and capable of developing into new hyphae.

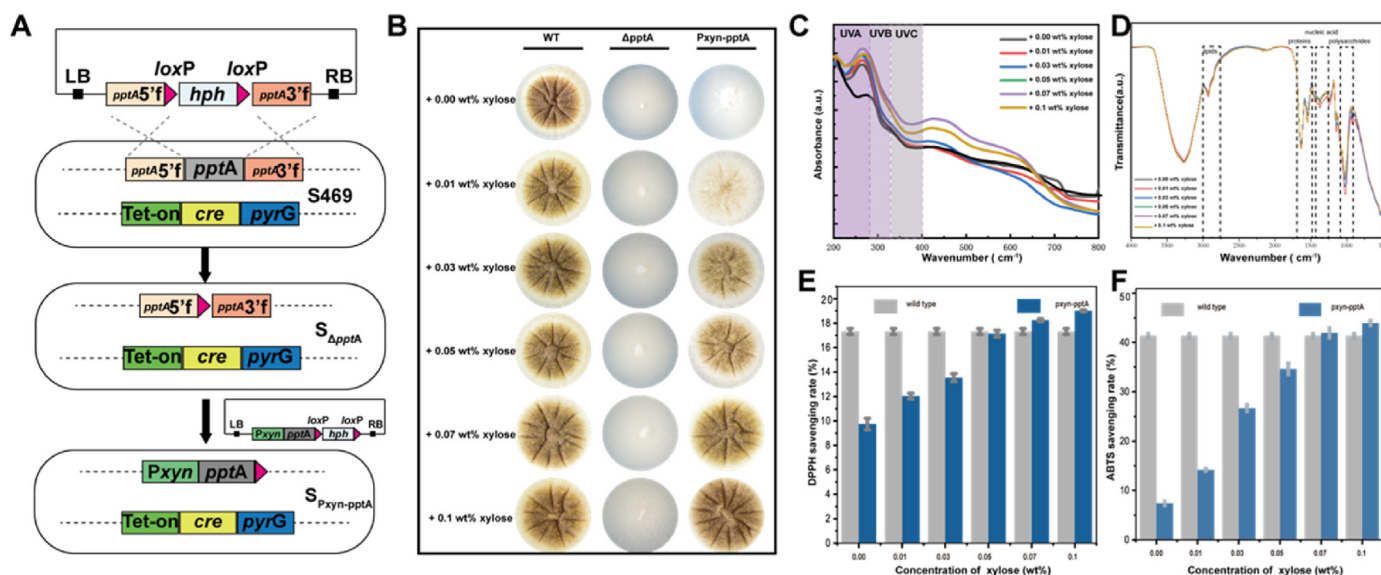


**Fig. 3.** Design and characterization of xylose-sensing living membrane materials based on the two *A. niger* strains. A, Schematic showing the construction of the  $\Delta$ pptA and Sp<sub>xyn-pptA</sub> strains for producing living membrane materials. 5'f and 3'f represent the upstream and downstream flanking sequences of *pptA* gene. RB and LB represent the right and left border sequences, respectively. B, The typical morphologies of living membrane materials grown from the wild type *A. niger* and the mutants ( $\Delta$ pptA, and Sp<sub>xyn-pptA</sub>), respectively. The indicated strains were cultured on PDA supplemented with different concentrations of 0.01, 0.03, 0.05, 0.07, and 0.1 wt% xylose for 3 days. C, UV-Vis spectra for the strain Sp<sub>xyn-pptA</sub> 0.01, 0.03, 0.05, 0.07, and 0.1 wt% xylose. D, ATR-FTIR spectra for induced with 0.01, 0.03, 0.05, 0.07, and.

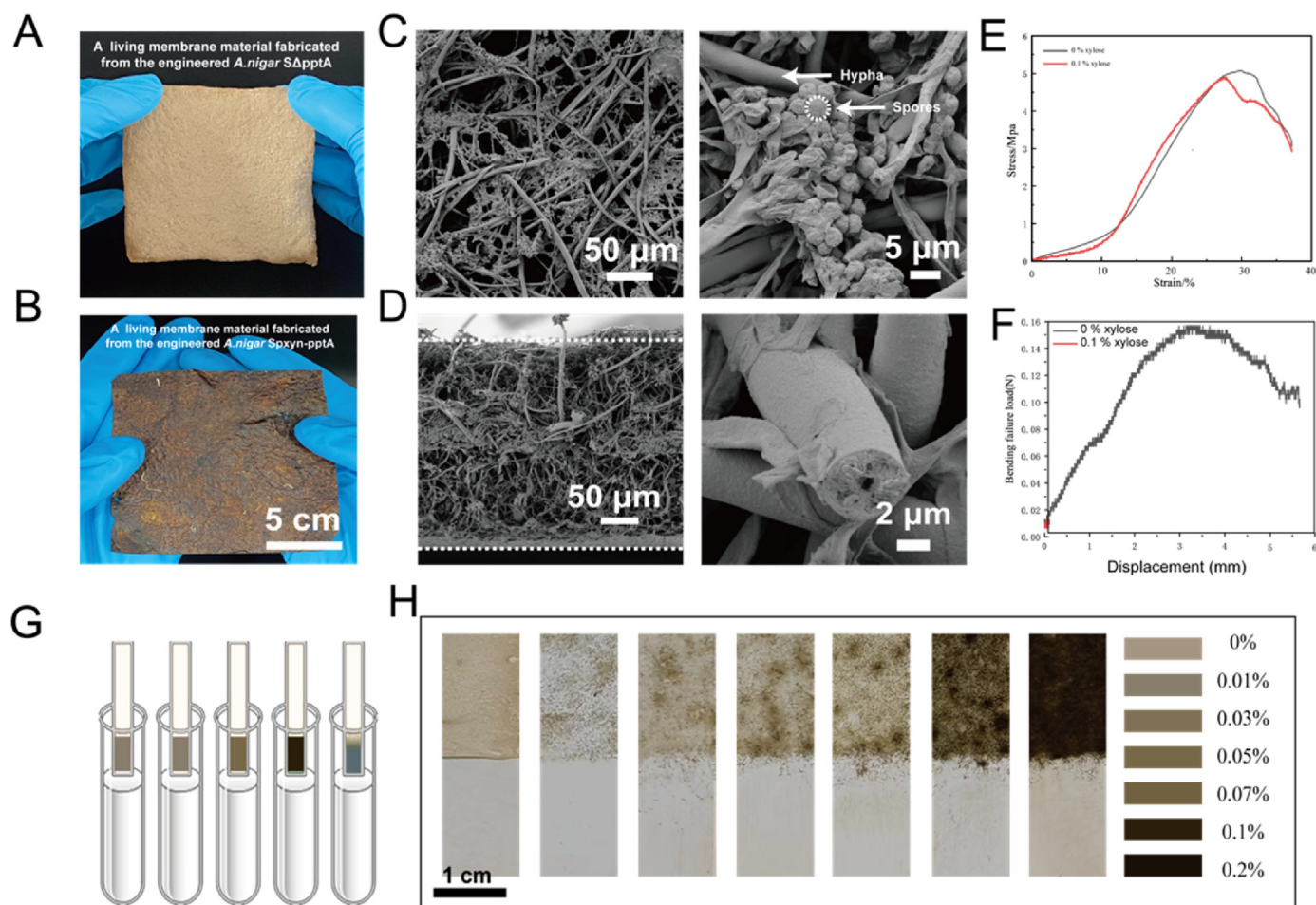


**Fig. 4.** Fabrication, physical, and structural characteristics of two different kinds of living membrane materials. A–D, Digital camera images (A–B) and SEM images (C–D) showing the surface morphology of living membrane materials grown from engineered *A. niger* SΔpptA and engineered *A. niger* Spxyn-pptA strains, respectively; E, representative stress/strain curves of living materials produced from engineered *A. niger* SΔpptA and Spxyn-pptA strains in the presence 0.1 wt% xylose added in culture media; F, Bending curve profile for living membrane materials grown from engineered *A. niger* SΔpptA and Spxyn-pptA strains in the presence of 0.1 wt % xylose added to culture media. G–H, schematic and digital images showing the tunable colors of selfdyed living membrane materials grown from engineered *A. niger* Spxyn-pptA strain, which secretes a controllable amount of melanin under different concentration of xylose. Note that the degree of color in turn reflects the amount of xylose concentration, implying a potential biosensor for detecting xylose in industrial waste. (For interpretation of the references to colour in this figure legend, the reader is referred to the Web version of this article.)

### 3.4. Xylose-responsive living membrane material for detecting xylose levels in wastewater

Given the accurate signal response of the engineered *A. niger*, we reasoned that the living cell-based pellets would function as building blocks that could then be used to produce living membrane materials with xylose-sensing ability. Xylose is the main component of hemicellulose hydrolysate [35], which is the papermaking wastewater produced by the pre-hydrolysis step. We hypothesize that the living membrane materials with variable colors in response to different concentrations of xylose may serve as a biosensor for detecting the xylose concentration in the papermaking wastewater.

To verify the potential application of living membrane material for wastewater testing, we cultured the material into a series of gradient dilutions of hemicellulose hydrolysate (composed mainly of xylose; 30 wt %), which was obtained from ground corn cobs after diluting hydrochloric acid hydrolysis at 100 °C for 2 h (Fig. 4G). Digital photographs showed that the degree of color could indeed reflect the difference in xylose concentration (Fig. 4H and Fig. S8). This successful demonstration of living membrane materials with tunable color gradients indicates that the living materials composed of live cells could behave as functional entities capable of responding to a realistic scenario.

Finally, because our living membrane material is composed of living cells, we evaluated its self-regeneration capacity and long-term viability. When partial fragments (~3 mg) of induced material were introduced into the culture media, the cells of the material started to re-proliferate to form new clumps (Fig. 5A and B). After 48 h of culture, the second generation (Gen II) living membrane material could regenerate from the fragments of the first generation (Gen I) living membrane material (Fig. 5C). Notably, The Gen II living membrane material was able to sense and respond to xylose. Moreover, we found that our material stored for 3 months at 4 °C could be used for regeneration in a fresh agar plate. No significant difference was found in terms of cell morphology, implying the possibility of long-term conservation of living membrane material. Moreover, these results demonstrate that these fabricated living membrane materials remain alive, self-regenerative, and functional.

## 4. Conclusion

Mycelium composites are an emerging class of cheap and environmentally sustainable materials experiencing increasing research interest for diverse applications, such as bovine leather and its substitutes, synthetic foams for packaging, insulation, and textiles, as well as high-performance paper-like materials [20,36]. Previous studies showed

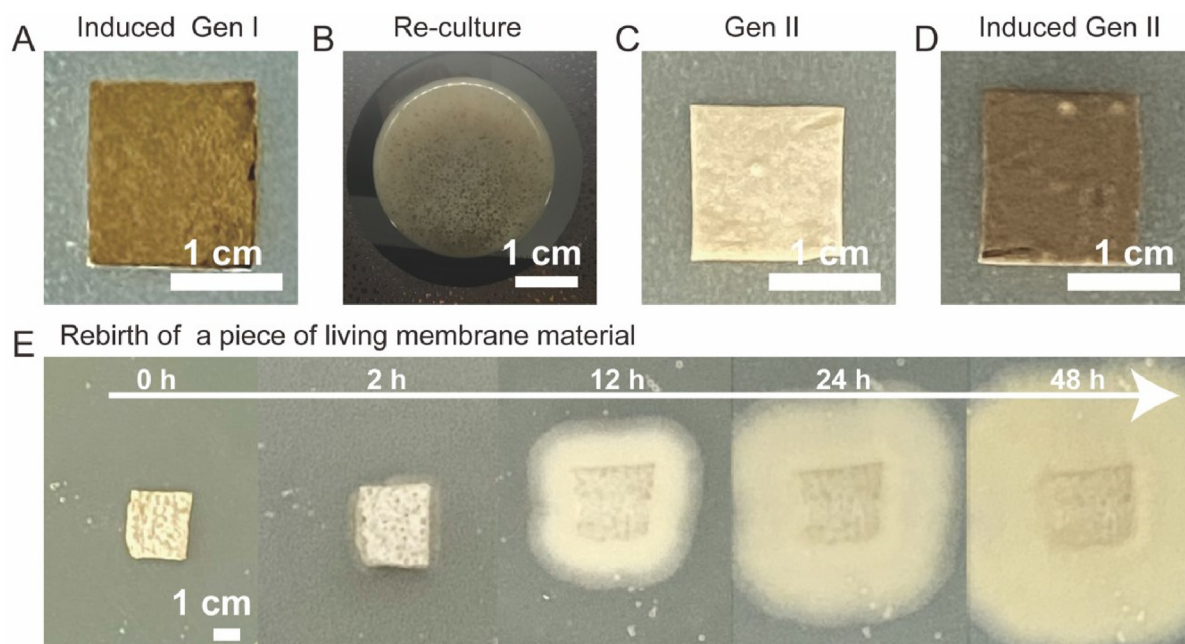


**Fig. 5.** Self-regeneration of living membrane materials. (A–D) Optical images of selfregeneration of living membrane material on agar plates for two continuous generations. From left to right: the xylose-induced first generation of living membrane material (GenI), partial fragments (~3 mg) of the induced (GenI) cultured in media, the second generation of living membrane material (GenII), the xylose-induced GenII. (E) The regeneration of a piece of living membrane material stored for 3 months at 4 °C in a fresh agar plate.

considerable promise in the fabrication of various materials using fungal mycelium. Nonetheless, some of these approaches face major obstacles, including the high-temperature processing steps and heavy reliance on strong chemical treatments during processing [20,36], leading to the death of living cells. Moreover, cells were required to be killed under certain circumstances, such as in food preservation. Living organisms exhibit remarkable environmental responsiveness to a variety of external stimuli and thereby provide an attractive opportunity for the development of dynamic functional materials. Hence, as a conceptual design, we constructed bulk ELMs with tunable colors and envisioned that this material could be developed with many other applications in further studies.

By leveraging the power of genetic engineering and the intrinsic advantage of the environmental tolerance of *A. niger*, we introduced a new type of engineered living material that enables tunable melanin production. Our self-supporting living membrane material made of genetically programmable living cells for environmental responsiveness has opened the door to creating fungi-derived materials with adaptive self-regeneration, as well as other previously unattainable material properties such as low pH resistance and accurate signal response.

Beyond the tunable properties that we demonstrated for our living membrane material, *A. niger* may be genetically engineered further for optimization using directed evolution methods. Thus, researchers can introduce various fused domains in conjunction with other materials to form composite materials with an even wider range of properties, such as responses to different inputs, including chemical inducers, pH changes, or temperature. However, as conidia eventually shed from the conidiophore and disperse into the air to maintain the colors of ELM, it is desirable to develop effective solutions to prevent the uncontrollable release of conidia in the environment. For instance, *A. niger* can be engineered with specific genetic circuits, which regulate the growth and survival of the conidia under specific nutrient contents [37]. Alternatively, a transparent, robust polymer-based coating can be developed and applied to maintain the colors of materials, preventing the conidia from escaping into the surroundings [38]. These efforts, in addition to

advances in biomanufacturing technology and synthetic biology, will facilitate the production of fabric, packaging, and biosensors.

#### Author contributions

K. Li: Conceptualization, Methodology, Investigation Validation, Formal analysis, Writing - Original Draft, Funding acquisition. Z. Wei: Methodology, Resources, Formal analysis, Writing - Original Draft. J.J. Jia: Methodology, Formal analysis. Q. Xu: Formal analysis, Resources. H. Liu: Validation, Resources. Formal analysis, Writing - Original Draft, Writing Review & Editing, Supervision. C. Zhong: Conceptualization, Writing Review & Editing, Supervision, Funding acquisition. H. Huang: Conceptualization, Writing Review & Editing, Supervision.

#### Funding

This work was supported by the China Postdoctoral Science Foundation (2021M690081) and received financial support from the National Key R&D Program of China (grant no. 2020YFA0908100 and 2018YFA0902804).

#### Declaration of competing interest

The authors declare that they have no known competing financial interests or personal relationships that could have appeared to influence the work reported in this paper.

#### Data availability

No data was used for the research described in the article.

#### Acknowledgments

The authors would like to thank the Shiyanjia lab (<http://www.shiyanjia.com/>) for the SEM imaging.

## Appendix A. Supplementary data

Supplementary data to this article can be found online at <https://doi.org/10.1016/j.mtbio.2023.100545>.

0.1 wt% xylose. E-F, DPPH and ABTS assay of Spxyn-pptA induced with 0.01, 0.03, 0.05, 0.07, and 0.1 wt% xylose. Data represent means  $\pm$  SD of three independent replicates. Statistical significance was determined by Student's *t*-test ( $n = 5$ ).

## References

- [1] A.Y. Chen, C. Zhong, T.K. Lu, Engineering living functional materials, *ACS Synth. Biol.* 4 (1) (2015) 8–11.
- [2] T. Liu, Y.Y. Yu, X.P. Deng, C.K. Ng, B. Cao, J.Y. Wang, S.A. Rice, S. Kjelleberg, H. Song, Enhanced *Shewanella* biofilm promotes bioelectricity generation, *Biotechnol. Bioeng.* 112 (10) (2015) 2051–2059.
- [3] R.S.H. Smith, C. Bader, S. Sharma, D. Kolb, T.-C. Tang, A. Hosny, F. Moser, J.C. Weaver, C.A. Voigt, N. Oxman, Hybrid living materials: digital design and fabrication of 3D multimaterial structures with programmable biohybrid surfaces, *Adv. Funct. Mater.* 30 (7) (2020).
- [4] T.-C. Tang, B. An, Y. Huang, S. Vasikaran, Y. Wang, X. Jiang, T.K. Lu, C. Zhong, Materials design by synthetic biology, *Nat. Rev. Mater.* 6 (2021) 332–350.
- [5] J. Huang, S. Liu, C. Zhang, X. Wang, J. Pu, F. Ba, S. Xue, H. Ye, T. Zhao, K. Li, Biofilms as engineered living materials, *Nat. Chem. Biol.* 15 (2019) 34–41.
- [6] C. Gilbert, T.-C. Tang, W. Ott, B.A. Dorr, W.M. Shaw, G.L. Sun, T.K. Lu, T. Ellis, Living materials with programmable functionalities grown from engineered microbial co-cultures, *Nat. Mater.* 20 (2021) 691–700.
- [7] Z. Guo, J.J. Richardson, B. Kong, K. Liang, Nanobiohybrids: materials approaches for bioaugmentation, *Sci. Adv.* 6 (12) (2020).
- [8] M. Schaffner, P.A. Ruhs, F. Coulter, S. Kilcher, A.R. Studart, 3D printing of bacteria into functional complex materials, *Sci. Adv.* 3 (12) (2017).
- [9] X. Liu, H. Yuk, S. Lin, G.A. Parada, T.-C. Tang, E. Tham, C. de la Fuente-Nunez, T.K. Lu, X. Zhao, 3D printing of living responsive materials and devices, *Adv. Mater.* 30 (4) (2018).
- [10] F. Fu, L. Shang, Z. Chen, Y. Yu, Y. Zhao, Bioinspired living structural color hydrogels, *Sci. Robotics* 3 (16) (2018) eaar8580.
- [11] K.T. Walker, V.J. Goosens, A. Das, A.E. Graham, T. Ellis, Engineered cell-to-cell signalling within growing bacterial cellulose pellicles, *Microb. Biotechnol.* 12 (4) (2019) 611–619.
- [12] C. Gilbert, T. Ellis, Biological engineered living materials: growing functional materials with genetically programmable properties, *ACS Synth. Biol.* 8 (1) (2019) 1–15.
- [13] C.M. Heveran, S.L. Williams, J. Qiu, J. Artier, M.H. Hubler, S.M. Cook, J.C. Cameron, W.V.S. Iii, Biomaterialization and successive regeneration of engineered living building materials, *Matter* 2 (2) (2020).
- [14] C. Zhang, J. Huang, J. Zhang, S. Liu, M. Cui, B. An, X. Wang, J. Pu, T. Zhao, C. Fan, Engineered *Bacillus subtilis* biofilms as living glues, *Mater. Today* 28 (2019) 40–48.
- [15] M. Haneef, L. Ceseracciu, C. Canale, I.S. Bayer, J.A. Heredia-Guerrero, A. Athanassiou, Advanced materials from fungal mycelium: fabrication and tuning of physical properties, *Sci. Rep.* 7 (2017), 41292.
- [16] M. Haneef, L. Ceseracciu, C. Canale, I.S. Bayer, J.A. Heredia-Guerrero, A. Athanassiou, Advanced materials from fungal mycelium: fabrication and tuning of physical properties, *Sci. Rep.* 7 (1) (2017), 41292.
- [17] M. Jones, A. Mautner, S. Luenco, A. Bismarck, S. John, Engineered mycelium composite construction materials from fungal biorefineries: a critical review, *Mater. Des.* 187 (2020), 108397.
- [18] C. Zhong, T. Gurry, A.A. Cheng, J. Downey, Z. Deng, C.M. Stultz, T.K. Lu, Strong underwater adhesives made by self-assembling multi-protein nanofibres, *Nat. Nanotechnol.* 9 (10) (2014), 858866.
- [19] M. Jones, A. Gandia, S. John, A. Bismarck, Leather-like material biofabrication using fungi, *Nat. Sustain.* 4 (1) (2021) 9–16.
- [20] A. Gandia, J.G. van den Brandhof, F.V.W. Appels, M.P. Jones, Flexible fungal materials: shaping the future, *Trends Biotechnol.* 39 (12) (2021) 1321–1331.
- [21] N. Yousefi, M. Jones, A. Bismarck, A. Mautner, Fungal chitin-glucan nanopapers with heavy metal adsorption properties for ultrafiltration of organic solvents and water, *Carbohydr. Polym.* 253 (2021), 117273.
- [22] D.P. Birnbaum, A. Manjula-Basavanna, A. Kan, N.S. Joshi, Hybrid living capsules autonomously produced by engineered bacteria, 2020.11, *bioRxiv* 23 (2020), 394965.
- [23] Y. Xu, L. Shan, Y. Zhou, Z. Xie, A.S. Ball, W. Cao, H. Liu, Development of a Cre-loxP-based genetic system in *Aspergillus Niger* ATCC1015 and its application to construction of efficient organic acid-producing cell factories, *Appl. Microbiol. Biotechnol.* 103 (19) (2019) 8105–8114.
- [24] W. Cao, L. Yan, M. Li, X. Liu, Y. Xu, Z. Xie, H. Liu, Identification and engineering a C4dicarboxylate transporter for improvement of malic acid production in *Aspergillus niger*, *Appl. Microbiol. Biotechnol.* 104 (22) (2020) 9773–9783.
- [25] C.B. Michiels, P.J.J. Hooykaas, C.A.M.J.J. van den Hondel, A.F.J. Ram, Agrobacterium-mediated transformation as a tool for functional genomics in fungi, *Curr. Genet.* 48 (1) (2005) 1–17.
- [26] C. Li, J. Zhou, G. Du, J. Chen, S. Takahashi, S. Liu, Developing *Aspergillus Niger* as a cell factory for food enzyme production, *Biotechnol. Adv.* 44 (2020), 107630.
- [27] M. Papagianni, Fungal morphology and metabolite production in submerged mycelial processes, *Biotechnol. Adv.* 22 (3) (2004) 189–259.
- [28] A. Gandia, J.G. van den Brandhof, F.V. Appels, M.P. Jones, Flexible fungal materials: shaping the future, *Trends Biotechnol.* 39 (12) (2021) 1321–1331.
- [29] R.M. McBee, M. Lucht, N. Mukhitov, M. Richardson, T. Srinivasan, D. Meng, H. Chen, A. Kaufman, M. Reitman, C. Munck, Engineering living and regenerative fungal–bacterial biocomposite structures, *Nat. Mater.* 21 (2022) 471–478.
- [30] T. Heinekamp, A. Thywissen, J. Macheleidt, S. Keller, V. Valiante, A. Brakhage, *Aspergillus fumigatus* melanins: interference with the host endocytosis pathway and impact on virulence, *Front. Microbiol.* 3 (2012) 440.
- [31] J.P. Latgé, R. Calderone, The fungal cell wall, in: U. Kues, R. Fischer (Eds.), *Growth, Differentiation and Sexuality*, Springer Berlin Heidelberg, Berlin, Heidelberg, 2006, pp. 73–104.
- [32] M.-K. Lee, N.-J. Kwon, I.-S. Lee, S. Jung, S.-C. Kim, J.-H. Yu, Negative regulation and developmental competence in *Aspergillus*, *Sci. Rep.* 6 (1) (2016), 28874.
- [33] N.C. McCallum, F.A. Son, T.D. Clemons, S.J. Weigand, K. Gnanasekaran, C. Battistella, B.E. Barnes, H. Abeyratne-Perera, Z.E. Siwicki, C.J. Forman, X. Zhou, M.H. Moore, D.A. Savin, S.I. Stupp, Z. Wang, G.J. Vora, B.J. Johnson, O.K. Farha, N.C. Gianneschi, Allomelanin: a biopolymer of intrinsic microporosity, *J. Am. Chem. Soc.* 143 (10) (2021) 4005–4016.
- [34] W. Cao, X. Zhou, N.C. McCallum, Z. Hu, Q.Z. Ni, U. Kapoor, C.M. Heil, K.S. Cay, T. Zand, A.J. Mantanona, A. Jayaraman, A. Dhinojwala, D.D. Deheyn, M.D. Shawkey, M.D. Burkart, J.D. Rinehart, N.C. Gianneschi, Unraveling the structure and function of melanin through synthesis, *J. Am. Chem. Soc.* 143 (7) (2021) 2622–2637.
- [35] E. Sjöman, M. Mänttari, M. Nyström, H. Koivikko, H. Heikkilä, Xylose recovery by nanofiltration from different hemicellulose hydrolyzate feeds, *J. Membr. Sci.* 310 (1) (2008) 268–277.
- [36] K. Li, J. Jia, N. Wu, Q. Xu, Recent advances in the construction of biocomposites based on fungal mycelia, *Front. Bioeng. Biotechnol.* 10 (2022).
- [37] A.J. Rovner, A.D. Haimovich, S.R. Katz, Z. Li, M.W. Grome, B.M. Gassaway, M. Amiram, J.R. Patel, R.R. Gallagher, J. Rinehart, F.J. Isaacs, Recoded organisms engineered to depend on synthetic amino acids, *Nature* 518 (7537) (2015) 89–93.
- [38] T.-C. Tang, E. Tham, X. Liu, K. Yehl, A.J. Rovner, H. Yuk, C. de la Fuente-Nunez, F.J. Isaacs, X. Zhao, T.K. Lu, Hydrogel-based biocontainment of bacteria for continuous sensing and computation, *Nat. Chem. Biol.* 17 (6) (2021) 724–731.